Title

Structural and functional connectivity of the human brain in autism spectrum disorders and attention-deficit/hyperactivity disorder: A rich club-organization study

Journal

Human Brain Mapping, 35(12)

ISSN

1065-9471

Authors

Ray, Siddharth
Miller, Meghan
Karalunas, Sarah
et al.

Publication Date

2014-12-01

DOI

10.1002/hbm.22603

Peer reviewed

◆ Human Brain Mapping 35:6032–6048 (2014) ◆

Structural and Functional Connectivity of the Human Brain in Autism Spectrum Disorders and Attention-Deficit/Hyperactivity Disorder: A Rich Club-Organization Study

Siddharth Ray,[1,2] Meghan Miller,[3] Sarah Karalunas,[4] Charles Robertson,[2] David S. Grayson,[2,5] Robert P. Cary,[2] Elizabeth Hawkey,[2] Julia G. Painter,[2] Daniel Kriz,[2] Eric Fombonne,[2,4,6,7] Joel T. Nigg,[2,4] and Damien A. Fair[2,4,8]*

[1]*Department of Diagnostic and Interventional Imaging, University of Texas Health Science Center, Houston, Texas*
[2]*Department of Behavioral Neuroscience, Oregon Health & Science University, Portland, Oregon*
[3]*Department of Psychiatry and Behavioral Sciences, University of California, Davis MIND Institute, Sacramento, California*
[4]*Department of Psychiatry, Oregon Health & Science University, Portland, Oregon*
[5]*Department of Psychiatry, Center for Neuroscience, University of California, Davis, Davis, California*
[6]*Department of Pediatrics, Oregon Health & Science University*
[7]*Institute of Development and Disability, Oregon Health & Science University*
[8]*Advanced Imaging Research Center, Oregon Health & Science University, Portland, Oregon*

Abstract: Attention-deficit/hyperactive disorder (ADHD) and autism spectrum disorders (ASD) are two of the most common and vexing neurodevelopmental disorders among children. Although the two disorders share many behavioral and neuropsychological characteristics, most MRI studies examine only one of the disorders at a time. Using graph theory combined with structural and functional connectivity, we examined the large-scale network organization among three groups of children: a group with ADHD (8–12 years, $n = 20$), a group with ASD (7–13 years, $n = 16$), and typically developing controls (TD) (8–12 years, $n = 20$). We apply the concept of the rich-club organization, whereby central, highly connected hub regions are also highly connected to themselves. We examine the brain into two different network domains: (1) inside a rich-club network phenomena and (2) outside a rich-club network phenomena. The ASD and ADHD groups had markedly different patterns of rich club and non rich-club connections in both functional and structural data. The ASD group exhibited higher connectivity in structural and functional networks but only inside the rich-club networks. These findings were replicated using the autism brain imaging data exchange dataset with ASD ($n = 85$) and TD

Additional Supporting Information may be found in the online version of this article.

Contract grant number(s): R01 MH096773 and K99/R00 MH091238 (to D. A. F.); Contract grant sponsor: Simons Foundation; Contract grant number(s): 177894 and R01 MH086654 and R01 MH86654 (to J. T. N.); Contract grant sponsor: Oregon Clinical and Translational Institute; Contract grant number: UL1TR000128 (to D. A. F.).

*Correspondence to: Damien Fair, Department of Behavioral Neuroscience, Oregon Health & Science University, Portland, OR.
E-mail: faird@ohsu.edu

Received for publication 30 October 2013; Revised 9 May 2014; Accepted 29 July 2014.

DOI: 10.1002/hbm.22603

Published online 13 August 2014 in Wiley Online Library (wileyonlinelibrary.com).

($n = 101$). The ADHD group exhibited a lower generalized fractional anisotropy and functional connectivity inside the rich-club networks, but a higher number of axonal fibers and correlation coefficient values outside the rich club. Despite some shared biological features and frequent comorbity, these data suggest ADHD and ASD exhibit distinct large-scale connectivity patterns in middle childhood. *Hum Brain Mapp 35:6032–6048, 2014.*

Key words: attention-deficit/hyperactivity disorder; autism spectrum disorders; high angular resolution diffusion imaging; rs-fMRI; connectivity; rich-club organization; DW-MRI; diffusion tensor imaging

INTRODUCTION

Attention-deficit/hyperactivity disorder (ADHD) and autism spectrum disorder (ASD) are two very common, costly, and impairing neurodevelopmental disorders. A recent study, surveying the years 1997–2008, concluded that one in six children in the United States have a developmental disorder, a 17% increase over the past decade driven largely by increases in ASD and ADHD [Boyle et al., 2011]. These trends highlight the need for innovative approaches to study these disorders.

Current diagnostic criteria for these disorders are based on clusters of signs and symptoms; ADHD is characterized by developmentally inappropriate levels of inattentive and/or hyperactive-impulsive behavior, while ASD is characterized by pervasive impairments in social communication and the presence of restricted interests and repetitive behavior [American Psychiatric Association, 2013]. However, despite clear differences in their formal diagnostic definitions, these phenotypes also show significant and intriguing overlap in terms of clinical comorbidity as well as in experimental findings. Unlike the *DSM-IV*, the *DSM*-5 [APA, 2013] allows codiagnosis of ADHD and ASD, in part because many children with ASD have impairing and comorbid inattention and/or hyperactivity [Rommelse et al., 2011]. This overlap extends to more specified executive functions as well, including set shifting, planning, and response inhibition [Geurts et al., 2004; Happé et al., 2006; Pennington and Ozonoff, 1996; Sinzig et al., 2008]. Furthermore, the two disorder's constituent symptoms appear to share some degree of common familial/genetic influences [Musser et al., 2014; Rommelse et al., 2010; Ronald et al., 2008].

As with various behavioral measures, studies of structural and functional brain connectivity in these two populations have provided initial insight into some noticeable overlaps in the functional and structural neuroanatomy of the disorders; however, findings have been somewhat inconsistent across studies. For example, structural evidence from diffusion tensor imaging studies (DTI) suggests reduced fractional anisotropy (FA)—a measure of white matter integrity [Mori and Zhang, 2006]—in both youth with ADHD and those with ASD, as revealed in parallel conclusions from recent meta-analyses of each conditions [Aoki et al., 2013; van Ewijk et al., 2012]. However, evidence of greater FA in specific regions including inferior parietal, occipitoparietal, inferior frontal, and inferior temporal cortex have been identified in both disorders as well [Cheung et al., 2009; Nagel et al., 2011; Silk et al., 2009]. Unfortunately, the two disorders have not been directly compared in regards to structural connectivity in the same study leaving it unclear if they actually differ in white matter development.

As with the structural literature, resting state functional connectivity studies in ADHD and ASD show apparent inconsistencies. Reduced connectivity between various brain regions have been identified in individuals with ADHD [Fair et al., 2010; Pavuluri et al., 2009; Peterson et al., 2009; Tomasi and Volkow, 2012; Uddin et al., 2008] and ASD [Anderson et al. 2011; Assaf et al., 2010; Cherkassky et al., 2006; Dinstein et al., 2011; Ebisch et al., 2011; Gotts et al., 2012; Kennedy and Courchesne, 2008; Monk et al., 2009; Mueller et. 2013; Rudie et al., 2012; von dem Hagen et al., 2012; Weng et al., 2010]. However, increased connectivity has also been identified in both disorders [Di Martino et al., 2011; Keown et al., 2013; Lynch et al., 2013; Monk et al., 2009; Supekar et al., 2013; Tien et al., 2006; Tomasi and Volkow, 2012; Uddin et al., 2013; Washington et al., 2014]. Again, direct comparison of the two disorders has been limited so it is unclear in what ways they have similar or distinct functional connectivity. Although recent studies by [Brieber et al., 2007] based on VBM, [Christakou et al., 2013] based on task-based fMRI, and [Di Martino et al., 2014] using functional network centrality measures have studied the two disorders in tandem, a comparison of large scale structural and functional network connectivity as measured via the "rich club" (see below for formal definition) has yet to be examined.

Overall, there is evidence that connectivity—both structural and functional—is disrupted in these two populations. In addition, although core diagnostic criteria for ASD do not overlap with those of ADHD, children with ASD often show high levels of inattention and hyperactive-impulsive symptoms, and individuals with ADHD often show deficits in one or more of the two primary ASD symptom domains (social communication impairments or restricted/repetitive behavioral patterns). To determine whether some of the shared behavioral patterns are the result of similar functional and/or structural neurophysiology, it is important to examine the disorders in the same study. Whereas many studies look at particular localized seed regions and their

connectivity, the evidence in both disorders of widespread alterations in connectivity commends an alternative approach. That is, it is important to consider the type and importance of a given connection identified in the context of the large-scale network structure of the brain, to clarify some of the inconsistencies reported in related literature. In this report, we use graph theoretical analyses of structural and functional connectivity to further our understanding of the underlying topological changes associated with ADHD and ASD diagnoses. Specifically, we examine structural, as well as functional, rich-club organization using high angular resolution diffusion imaging (HARDI) and resting state functional connectivity MRI (rs-fMRI) in children with ASD, in children with ADHD, and in typically developing children.

Recent work has proposed that rich-club organization may be a key topological property of the healthy human brain. The term "rich-club organization" refers to a system organization whereby highly connected nodes within a network (e.g., the brain) show a tendency to connect with other highly connected nodes; this concept has recently been applied to structural and functional networks in the healthy human brain and has indicated that the human brain indeed shows robust rich-club organization [van den Heuvel and Sporns, 2011]. These methods offer a novel way by which to examine atypical neural network organization in neurodevelopmental disorders, including ADHD and ASD, that integrates the organizational tendencies of the entire brain rather than attempting to isolate specific localized abnormalities. Such work carries implications for dissection of the inconsistencies inherent to the literature, discovery of potential underlying mechanisms, and identification of potential neural endophenotypes [see Rommelse et al., 2011], all of which could critically impact diagnostic and classification efforts. Studies have shown that the regions in the structural rich club include superior medial frontal/dACC, medial parietal/PCC, insula and inferior temporal cortex, while functional rich-club regions include areas in midline frontal, midline posterior, insula, inferior temporal, and cingulate cortex [Grayson et al., 2014; van den Heuvel and Sporns, 2011]. In this study, we anticipate atypical structural and functional connectivity patterns amongst these rich-club regions in both ADHD and ASD groups, and that the nature of these connectivity patterns will persist with both functional and structural data within each group.

MATERIALS AND METHOD

Participants

The study sample consisted of children aged 7–13 years, including 20 typically developing controls (TD), 20 children with ADHD (includes 8 inattentive, 1 hyperactive, and 11 combined type by DSM-IV criteria), and 16 high-functioning-ASD children [Supporting Information Table 1(a)]. All ADHD participants were recruited by community outreach and were diagnosed by a research diagnostic team that included a licensed psychologist, board certified child psychiatrist, and licensed clinical social worker using consensus review based on a semistructured clinical interview [K-SADS; Kaufman et al., 1997] and parent and teacher standardized ratings. The ASD children were recruited from referrals to a tertiary autism treatment center. For ASD participants, diagnosis was determined by a multidisciplinary clinical team that utilized the ADOS [Lord et al., 2000]. All children also met ASD criteria on the ADI-R [Lord et al., 1994], using *DSM-IV* criteria [American Psychiatric Association, 2000]. Children with ASD were assessed for ADHD by the same research methods [Supporting Information Table 1(b)]; 16 children with ASD also had a diagnosis of ADHD. Typically developing control children (TD) were recruited as community volunteers. They underwent the same diagnostic evaluation as the youth in the ADHD cohort, including review of semi-structured clinical interview and parent and teacher standardized rating forms by the ADHD diagnostic team to ensure they did not meet criteria for ADHD or ASD.

Exclusion criteria for all groups included neurological disorder, seizure disorder, cerebral palsy, pediatric stroke, history of chemotherapy, sensorimotor handicaps, closed head injury, thyroid disorder, schizophrenia, bipolar disorder, current major depressive episode, fetal alcohol syndrome, Tourette's disorder, severe vision impairments, Rett's syndrome, and IQ $>$ 70. Children with ADHD or ASD who were taking psychostimulant medications were allowed in but were washed out for a minimum of 24–48 hours (depending on formulation) or at least 7 half lives of the formulation (i.e., the period of time it takes the body to metabolize/excrete half of the dose of the medication) prior to neuroimaging. This action was verbally confirmed with parents. Children taking nonstimulant psychoactive medications (e.g., tricyclic antidepressants, SSRIs, MAO inhibitors, or antipsychotic medication and atomoxetine) were excluded from the study. Typically developing children were all free of psychoactive medication.

Data Acquisition

MR data were collected during a single session for each subject using a Siemens Tim Trio 3T Scanner with a 12-channel head coil. Data acquisition included: (1) T1-weighted magnetization-prepared gradient-echo image [repetition time (TR) = 2,300 ms, inversion time (TI) = 900 ms, echo time (TE) = 3.58 ms, flip angle (FA) = 10°, 1 mm^3 voxels, 160 slices, FOV = 240 × 256 mm]; (2) T2-weighted image for accurate registration of T1-weighted over b0 (TR = 3200 ms, TE = 497 ms; 1 mm^3 voxels, 160 slices, FOV = 256 × 256 mm); (3) HARDI using an Echo Planar Imaging (EPI) (72 different gradient directions, *b*-value = 3,000 mm/s^2, TR = 7100 ms, TE = 112 ms, 2.5 mm^3 voxels, 48 slices, FOV = 230 × 230 mm) and (4) resting-state functional MRI (*rs-f*MRI) using a gradient-echo echo-planar imaging (EPI) sequence (TR = 2500 ms, TE = 30 ms, FA = 90°, 3.8 mm^3volexs, 36 slices with interleaved

acquisition, FOV = 240 × 240 mm). We acquired three 5-min runs, making total of 15 min of resting state data for each subject in the study.

T1 preprocessing

For each dataset, the T1-weighted images were used as anatomical references to identify regions of interest (ROIs) in the brain network. Freesurfer (http://surfer.nmr.mgh.harvard.edu/), was used to classify white/gray matter tissue and to parcellate the cortical gray matter into 68 regional labels in native space. These regions were further subdivided into 219 [Hagmann et al., 2008] equivalent size cortical ROIs (using connectomemapper: http://www.connectomics.org/connectomemapper/). This region set was obtained from each subject after its surface registration, which is required for proper tractography and ensuring the validity of comparisons between different subject groups.

HARDI Quality Assurance

Despite investigators best efforts, poor image quality is not uncommon in MRI studies, particularly with awake, pediatric populations. In view of the large number of images acquired during each patient session, manual examination of all the images for quality assurance is often time-consuming and prone to human error. Instead, we used MATLAB script to implement a pipeline to automatically identify the images with suboptimal quality. Each subject's HARDI data went through the steps of this pipeline, which was based on frame-to-frame and slice-to-slice intensity matching. The program reads the whole digital imaging and communication in medicine volume and flags the frames with unacceptably low signal intensity value compared to other frames in the same volume. Here, frames with difference in signal intensity, from mean of intensities, greater than threshold_1 and with difference in signal intensity, from the maximum intensity, greater than threshold_2 were considered suboptimal quality frames. This can be equated as:

$$\text{Frame}_{\text{sub-optimal}} \rightarrow (\boldsymbol{F}_{\text{mean}} - \boldsymbol{F}_i) > \text{thresh}_1 \,\&\, (\boldsymbol{F}_{\text{max}} - \boldsymbol{F}_i) > \text{thresh}_2 \quad (1)$$

Here, F_{mean} represents the mean of all frames intensities, F_i represents the intensity of the ith frame under consideration, F_{max} represents the maximum intensity of the frame and thresh_1 and thresh_2 represents threshold values that were empirically chosen.

The routine then selects the flagged frames and flags the slices with unacceptably low signal value compared to the other slices in that frame, in the same way. These flagged frames and slices were then manually examined and all datasets with suboptimal image quality, that is, dataset with more than five flagged frames (threshold_1) and five flagged slices (threshold_2), were excluded from the study. After exclusion for motion, the final n for HARDI analysis was 20 TD, 20 ADHD, and 8 ASD subjects. There were no significant differences in age (p-value = 0.8) and IQ (p-value = 0.08) between the eight ASD subjects included and eight ASD subjects excluded after quality assurance.

HARDI Preprocessing and Tractography

Diffusion data processing was then performed using connectomemapper and included four main steps, as outlined below.

Coregistration of the T1-weighted image and b0 image

This step was performed using the T2-weighted image as an intermediary, first applying a rigid body transformation of the T1-weighted image over the T2-weighted image, and then a nonlinear registration between the T2-weighted image and the b0 image. The additional step of nonlinear registration allowed us to account for distortions introduced by susceptibility artifact and eddy currents. Skull stripping on the b0 and T2-weighted images was performed prior to nonlinear coregistration, to ensure the robustness of the algorithm.

HARDI reconstruction

Data reconstruction in HARDI was done using a Q-Ball scheme [Tuch, 2004]. The diffusion data were resampled into 2 mm^3 voxel size and were reconstructed by defining the orientation distribution function (ODF) for each voxel. These ODFs were defined using a tessellated sphere of 181 vertices, each representing the estimated diffusion in that direction. Up to three directions of diffusion were defined using local maxima of the ODF.

Tractography

Using the extracted information from ODF within each voxel, 32 evenly spaced fibers were initiated along every direction of maximum diffusion orientation. All fibers were propagated in back-forth directions, and continued along the diffusion direction on reaching a new voxel. The fiber tracking was continued unless change in tracking direction was $>60^\circ$ or the tracking left the white matter mask. In addition, fiber streamlines of length <20 mm were considered potentially spurious and were removed.

Connections matrix

Connections between the ROIs were identified using the results from the tractography and gray matter parcellation. Two ROIs, ROI1 and ROI2, were said to be connected if a fiber originated from either of the ROIs (e.g., ROI1) and terminated in the other ROI (e.g., ROI2). The connections were weighted by the total number of streamlines between the two ROIs, and streamlines were included only if the

two-end points were in ROI1 and ROI2. The final outcome was a symmetric, weighted, and undirected connection matrix of size 219 × 219 with cell values signifying the number of streamlines between the ROI pairs.

Generalized fractional anisotropy mean

FA, in a diffusion process, is the degree of anisotropy within a voxel, with values ranging between 0 and 1. An analogous measure in HARDI (q-space imaging) is generalized fractional anisotropy (GFA), and is defined as a measure of variation in diffusion ODF [Tuch, 2004]. GFA, using ODF, gives a better estimation of anisotropy than FA in DTI, detecting multiple fiber pathways [Cohen et al., 2008]. GFA-mean values, calculated as the mean of GFA-values within all the voxels along all the fiber trajectories between the two ROIs, were computed for each parcellated ROI pair. The end result was a 219 × 219 symmetric matrix where each cell value signifies the GFA-mean value between the ROI pairs.

fMRI Preprocessing and Connectivity

The preprocessing of fMRI data includes slice-time correction, debanding, motion-correction, registration onto the T1 image, and resampling into 3 mm^3 voxel size. In addition, temporal bandpass filtering ($0.009\ Hz < f < 0.08\ Hz$), spatial smoothing (6 mm full-width at half-maximum), and regression of nuisance signals (i.e., global, CSF, and white matter) were also performed [Fox et al., 2005]. The nuisance regressors were generated and applied after the bandpass filter consistent with recommendations by Hallquist et al. [2013].

Motion censoring

Every subject went through the following steps for head motion correction. First, for every time point frame-to-frame displacement was calculated as a scalar quantity, given by sum of frame-wise displacement (FD) in six rigid body parameters [Power et al., 2012]. At each time point, the current frame with one preceding and two following frames were excluded if the FD was greater than 0.3 mm [Power et al., 2012]. Furthermore, subjects with more than 50% of frames removed were excluded from the study [see Fair et al., 2013] and, thus, each dataset had at least 5 min of BOLD data remaining. On this basis, one control and one ADHD subject were excluded from further analysis leaving a final n for functional connectivity of 19 ADHD, 16 ASD, and 19 TD (with no significant differences in age and IQ between groups). Of the remaining samples, average frame removal in TD was 24% ± 20.08% (mean ± SD), in ADHD was 20% ± 18.88% and in ASD was 29% ± 20.61% (Supporting Information Table 2). The average time remained in TD, ADHD, and ASD were 11, 11.1, and 8.67 min, respectively.

Autism brain imaging data exchange dataset

A second dataset was used for cross validation, called the autism brain imaging data exchange (ABIDE) dataset [Di Martino et al., 2014] TD ($n = 114$) and ASD subjects ($n = 104$) 7–14 years of age and with $IQ > 70$ were selected for the functional connectivity analysis. Standard processing (same as above) was done for each dataset. After correcting for motion, 13 TD and 19 ASD subjects were excluded, leaving 101 TD and 85 ASD subjects (Supporting Information Table 3). This dataset did not include any participants from the OHSU site.

Connections matrix

For each of the cortical ROIs, time series were computed by averaging the signal intensity across all voxels within the ROI for each time point. Next, cross-correlations were computed between the time series of all ROI pairs, yielding a correlation value between −1 and 1 for each pair. The final result was a 219 × 219-size correlation matrix for each subject.

Masking Adjacent Connections

In both structural and functional data, connectivity shows a predominance to local and short-range connections. Although biological aspects of these phenomena are important, they often have artifactual contributions when measuring the connectivity of the network. In functional data, preprocessing steps (e.g., signal blurring) and head movement causes nonbiological signals in the neighboring voxels. In structural data, long-range fibers are more likely terminated due to noise.

To ensure our findings were not determined by this potential artifact, analyses were conducted on the original matrices and a matrices constructed by excluding connections between all neighboring ROIs. Additionally, all the structural connections with fiber lengths <30 mm were also excluded.

Group Networks

After computing the connection matrices for each subject in all three cohorts (TD, ADHD, and ASD), a group-averaged matrix was computed for both structural and functional connection matrices, by following these steps. For structural data, following prior publications, we took the following steps. From the set of individual group structural matrices (TD, n=20; ADHD, n=20; ASD, n=8), only connections that were present in at least 50% of population of a given group were selected for averaging, while all other connections were set to 0. The group-averaged matrix was then computed by averaging only across the non-zero cell values of the individual subject matrices. These steps were similar to the methods used by others [van den Heuvel and Sporns, 2011; van den Heuvel et al., 2012], and were considered useful for mitigating noise caused by intersubject variability. For functional

imaging data, the group-averaged matrix within each group (TD, $n=19$; ADHD, $n=19$; ASD, $n=16$) was computed by averaging the individual subject's correlation matrices together. To implement graph theory on the functional data, negative correlations were omitted, while for an unbiased comparison of graph metric between groups, group networks were thresholded to include only top 3% of the strongest positive correlation. However, we also validated the results within the range of 2%–9% connection densities.

GFA Analysis

Following the same rules of group network construction, a group-averaged matrix of GFA-mean values was computed and a vector of all non-zero values was reconstructed for each subject group. First, a one-way ANOVA was used to test for group differences in GFA-mean values. Next, two-sample *t*-tests were performed to identify which groups significantly differed in GFA values.

Graph Metrics and Analyses

We applied graph theory to analyze the structural and functional connectivity pattern in the TD, the ASD, and the ADHD groups. Each of the 219 cortical regions constitutes a node, connections between these nodes constitutes links, and number of streamlines (in structural)/correlation values (in resting state *fc*-MRI) constitutes weight/strength of the links. While the presence of streamlines determines the connection between ROIs in structural, the existence of functional connections was determined by the correlation values, with only top 3% of all correlation values considered as connections. Results were also tested at 6% and 9% connection density.

Rich-club organization

The rich-club organization was analyzed on both weighted structural and weighted functional matrices. The weighted rich-club coefficient (ϕ^w), at degree level of k, for a matrix was computed using equation [Colizza et al., 2006; Opsahl et al., 2008; van den Heuvel and Sporns, 2011; Zhou and Mondragon, 2004]:

$$\phi^{w}(k)=\frac{W_{>k}}{\sum_{l=1}^{E_{>k}} w_l^{\text{sorted}}} \tag{2}$$

Where $W_{>k}$ was the weighted sum of all connections $\geq k$ and the denominator was the sum of top $E_{>k}$ connection weights, sum of top weighted connections with degree $\geq k$, in the network. To identify the existence of the significant rich-club organization in the network, rich-club coefficients ϕ^wwere normalized relative to a set of 1,000 comparable random networks [Bassett and Bullmore, 2009; van den Heuvel et al., 2010]. In this study, these random matrices for the structural and functional data were created by randomizing the connections and at same time preserving the degree distribution and sequence of the matrix [Maslov and Sneppen, 2002]. The rich-club coefficients computed for each random matrix were averaged across all 1,000, denoted as $\phi^w_{\text{random}}(k)$. Weighted normalized rich-club coefficient $\phi^w_{\text{norm}}(k)$ was calculated by the equation:

$$\phi^{w}_{\text{norm}}(k)=\frac{\phi^{w}(k)}{\phi^{w}_{\text{random}}(k)} \tag{3}$$

In addition to the Maslov–Sneppen method for rewiring, mentioned above, we also used Hirschberger–Qi–Steuer (H-Q-S) algorithm, keeping the transitivity intact, described in [Zalesky et al., 2012], for normalizing the rich-club coefficient in the functional networks.

The network was said to have a rich-club organization when the normalized coefficient was greater than 1 for a range of k values. To analyze the statistical significance of the results, permutation testing [Bassett and Bullmore, 2009; van den Heuvel et al., 2010] was used. A null distribution using the rich-club coefficients from 1,000 random networks was used and a p-value was calculated for coefficient values $\phi(k)>\phi_{\text{random}}(k)$ as the percentage of $\phi_{\text{random}}(k)$ that exceeded $\phi(k)$. The p-values were assigned for each degree and those <0.05 were considered to have significantly higher rich-club coefficient values.

In this article, we extended the concept of rich-club organizations and separated the brain networks in two domains of connectivity defined using the rich-club phenomena. This helped us to analyze the specificity of over/under-connectivity in the structural and functional brain networks of the ASD and the ADHD groups. The two domains of connectivity were: (1) networks inside the rich-club organization and (2) networks outside the rich-club organization. The networks inside the rich-club organization were networks with regions that have at least k or more than k connections and networks outside the rich-club organization were networks with regions that have less than k connections. Graph metrics, measured in these two domains, were computed for a range of k values for both inside and outside the rich-club organization. For a better understanding and to avoid the redundancy in results, we used a higher k value range for inside and lower k value range for outside the rich-club organization.

Connectivity index (β)

The connectivity index is a simple measurement that represents the average number of connections per node in a given network and computed as the ratio of the total number of connection (E) to the total number of nodes (N). The term can be formulated as:

$$\beta=\frac{E}{N} \tag{4}$$

This term provides a level of network connectivity by measuring the network's complexity. Connectivity indices were computed for networks inside and outside the rich-club organization.

Connectedness coefficient (κ)

To compare the connectivity between two different sized brain networks is often not straightforward, as network connectivity is influenced by its number of nodes (N) and average degree (k), and, thus, comparison of graph metrics (such as clustering coefficient, connectivity index, path length, and participation coefficient) between networks can yield spurious results due to the N-k dependence [van Wijk et al., 2010]. To minimize the effect of size of the network, we implemented a novel graph metric, called connectedness coefficient, given by the product of the network's rich-club coefficient and its connectivity index. The rich-club coefficient is less influenced by larger networks where nodes have high chances to link with other nodes in the networks, while the connectivity index is less biased to smaller networks where the chances of having total number of connections to total number of possible connections is close to 1. Thus, the connectedness coefficient minimizes the network's N-k dependence and provides us with a more unbiased measurement to compare the structural and functional network connectivity between our three groups of subjects. To have a better understanding of connectedness coefficient, we have showed some small sample networks with rich-club coefficients, connectivity indices, and connectedness coefficients calculated (Supporting Information Fig. 1). Connectedness coefficients were measured for two different network domains of rich-club organization (refer result section).

The connectedness coefficient for unweighted (κ) and weighted (κ_w) matrices are given by the following equations, respectively:

$$\kappa = \frac{2E^2}{N^2(N-1)} \tag{5}$$

$$\kappa_w = \frac{W^2}{N.W_l^{\text{sorted}}} \tag{6}$$

Statistical significance

Differences in the connectedness coefficients between groups were tested for significance using two different methods: (1) permutation testing: for each i^{th} iteration of the group's random network M_{1i} M_{2i}, the difference between connectedness coefficients for M_{1i} and for M_{2i} yielded a null distribution of 1,000 random differences and (2) by randomizing labels between groups (Supporting Information Figs. 3–5): for each permutation, the first group contains a random mix of subjects from the second group and from its own group, and randomizations were done likewise for the second group. The difference in the coefficients were then computed for the new randomized networks, yielding a null distribution of 1,000 random differences. Using either of these distributions, a p-value was assigned to each observed difference as the percentage of random differences that exceeded the difference value and coefficients with p-value < 0.05 were considered significant.

RESULTS

As shown in Supporting Information Table 1(a), there was no statistically significant difference in age and full scale IQ between the three groups in the OHSU sample. The results from the primary analyses were then cross-validated using ABIDE dataset.

Structural

Higher rich-club organization in ASD group

We began our analyses by first identifying the structural rich-club organization in the three cohorts (ASD, TD, and

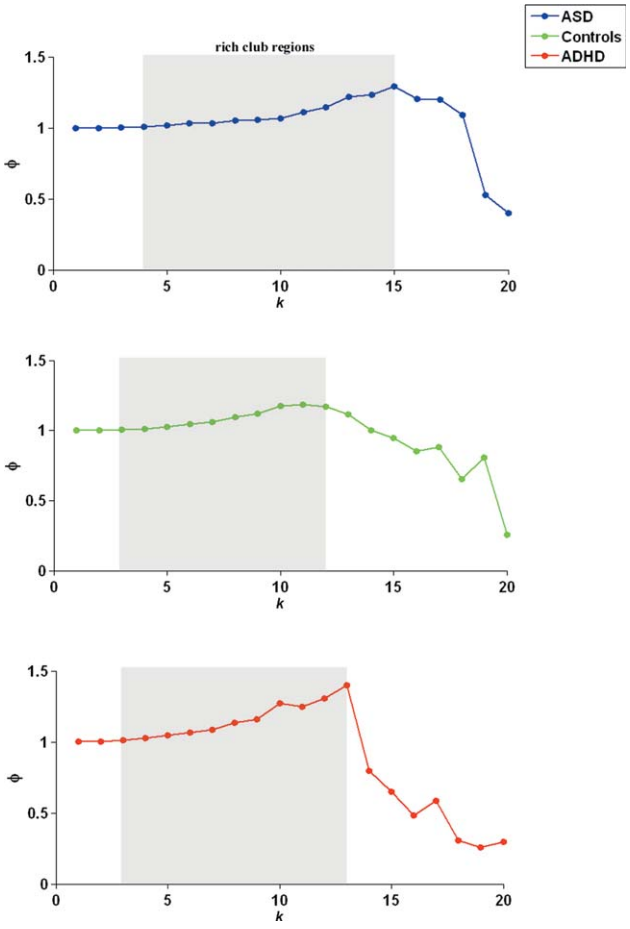

Figure 1.

Rich-club organization in structural group networks of ASD, TD, and ADHD. Rich-club coefficients normalized relative to random are shown in blue (ASD), green (controls), and red (ADHD) colors. The coefficients are plotted against degree, between 1 and 20. Shaded regions shows the significant ($p < 0.05$) higher coefficients.

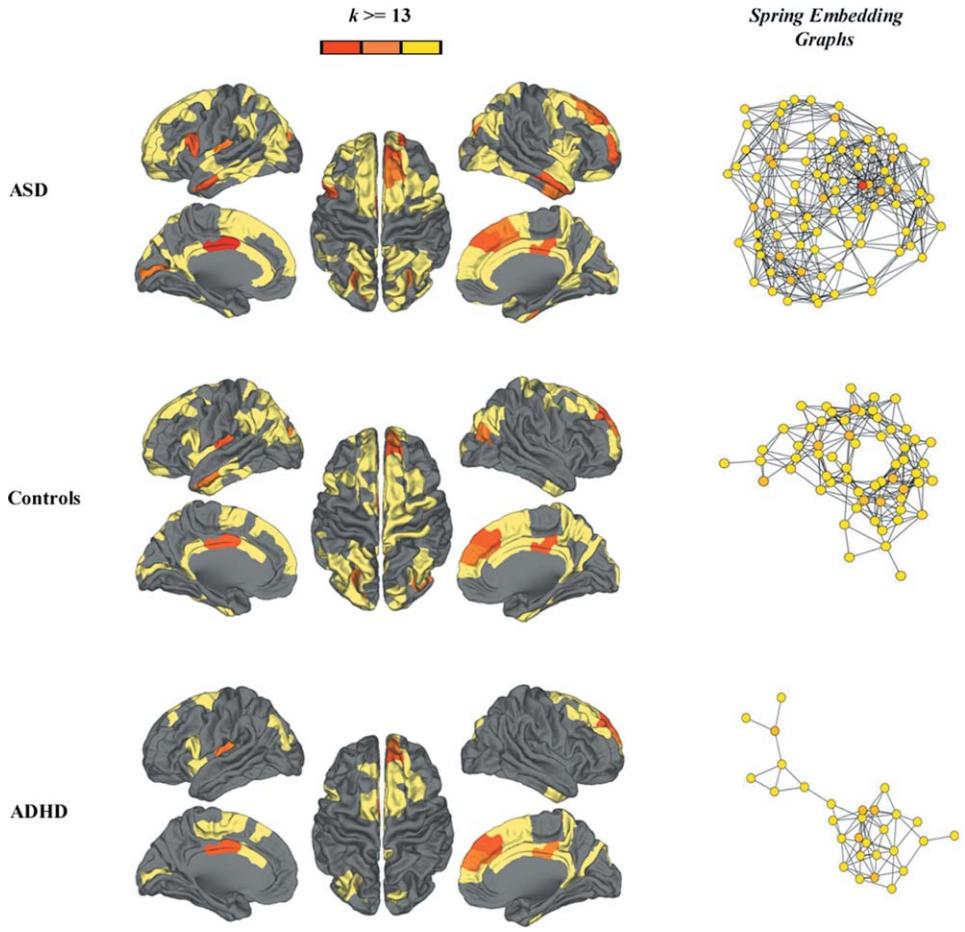

Figure 2.

Spatial topography and spring embedded graphs of structural rich club in ASD, control, and ADHD (top–bottom). Rich-club regions at $k \geq 13$ are shown for all the three groups. Regions are colored based on their degree distribution (yellow to red). On the right-hand side are the corresponding spring embedded graphs for each group where regions are depicted as circles and links between them are the solid lines between them.

ADHD). All three groups showed the existence of significant rich-club organization in their weighted structural connectivity network, shown in Figure 1. The regions comprising rich-club organization were distributed bilaterally and include anterior and posterior cingulate cortex, superior frontal, superior parietal, and insula cortex, as well as the inferior temporal for TD group. Children with ASD showed similar regions and extending more along anterior cingulate, superior frontal and inferior temporal cortex, while children with ADHD also showed similar regions but narrowing along superior frontal, posterior cingulate, inferior temporal, and superior parietal regions. From Figure 1, we observed that the rich-club organization in the ASD group existed for a higher value of k (degree) than in the ADHD or TD, indicating a higher number of connections in the ASD group. When compared for the difference in the ϕ_{norm} between groups, subjects with ASD showed significantly higher rich-club coefficients, at high k level than both the TD and ADHD, indicating over-connectedness between the rich-club nodes (Supporting Information Fig. 2). Figure 2 displays the brain pictures of the rich-club regions at $k \geq 13$ and the corresponding spring embedding graph showing these regions in the ASD, TD, and ADHD groups. As visualized in Figure 2, subjects with ASD showed more rich-club regions with over-connectedness among them than TD, while subjects with ADHD showed fewer rich-club regions with under-connectivity among them than the TD group.

High connectedness coefficient inside rich club for ASD group

To analyze whether the over-connectedness in the ASD and under-connectedness in the ADHD group, as seen

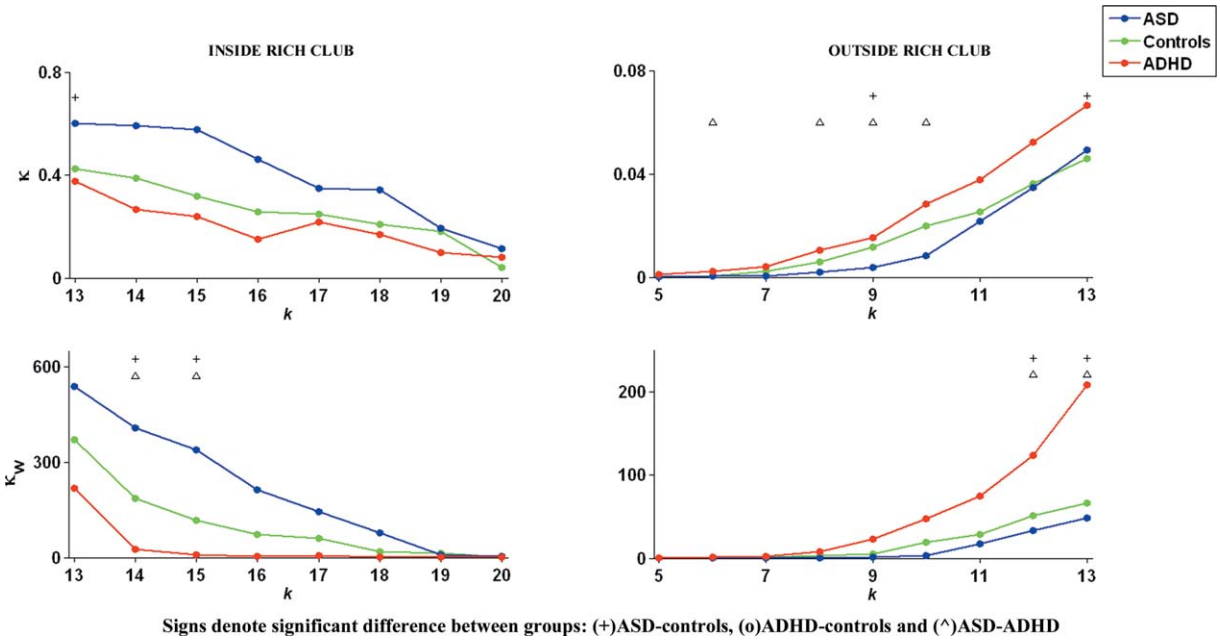

Figure 3.

Connectedness coefficients (unweighted and weighted) between structural networks of ASD, controls, and ADHD for networks inside and outside the rich-club organization. Graphs on the left-hand side show the unweighted connectedness coefficients and weighted coefficients comparison between groups inside the rich club ($13 \leq k \leq 20$), while right-hand *side* graphs shows these comparison for networks outside the rich club ($5 \leq k \leq 13$). Significant differences between ASD-controls are marked with "+" sign, ADHD-controls are marked with "o" sign, ASD-ADHD are marked with "^" sign.

from the spring embedded graph in Figure 2, were specific to rich-club regions or to a whole brain network, we next compared the unweighted and weighted connectedness coefficients among the three groups (Fig. 3), using the two domains mentioned above. We chose a range of $13 \leq k \leq 20$ for inside rich-club organization and range $5 \leq k \leq 13$ for outside the rich-club organization. Figure 3 shows graphs of unweighted and weighted connectedness coefficients plotted against k for networks inside and outside the rich-club organization. Subjects with ASD showed a significantly higher connectedness coefficient inside the rich-club organization than the TD and ADHD participants; however, we did not see any significant difference outside the rich-club organization. These findings suggest that the higher connectedness in the ASD group is specific to the rich-club regions. Significant differences for connectedness coefficients were also tested by randomizing group labels (Supporting Information Figs. 3–5). We observed significant reduced connectedness coefficients inside the rich club, while increased coefficients outside the rich club for children with ADHD (Supporting Information Fig. 4). Children with ASD showed higher connectedness coefficients inside the rich club, while and lower coefficients outside the rich-club organization (Supporting Information Fig. 3).

Lower GFA-mean in ADHD group and more streamlines in ASD group inside rich-club organization

To investigate the cause of over-connectedness in ASD group and under-connectedness in ADHD group inside rich-club organization, we analyzed white matter integrity using GFA-mean matrix, and the actual number of fiber streamlines in the ASD, ADHD, and TD groups. ANOVA performed on all non-zero GFA-mean values of all three groups showed reduced GFA values in the ADHD group, with no significant differences between the ASD and the TD groups (Supporting Information Fig. 6).

We next compared the ADHD and ASD groups GFA values in networks inside and outside the rich-club organization. GFA values of only those regions with $k \geq 13$ were analyzed for inside rich-club organization comparisons, while GFA values of only those regions with $k \leq 13$ were analyzed for outside rich-club comparisons. Two-tailed *t*-tests showed significantly reduced GFA-mean in the ADHD group inside the rich-club compared to the TD and the ASD groups (shown in Fig. 4), while there was no significant difference observed in GFA-mean values outside the rich-club organization. The reduced GFA-mean values in the ADHD group specific to rich-club organization suggest its association with the lower connectivity in ADHD.

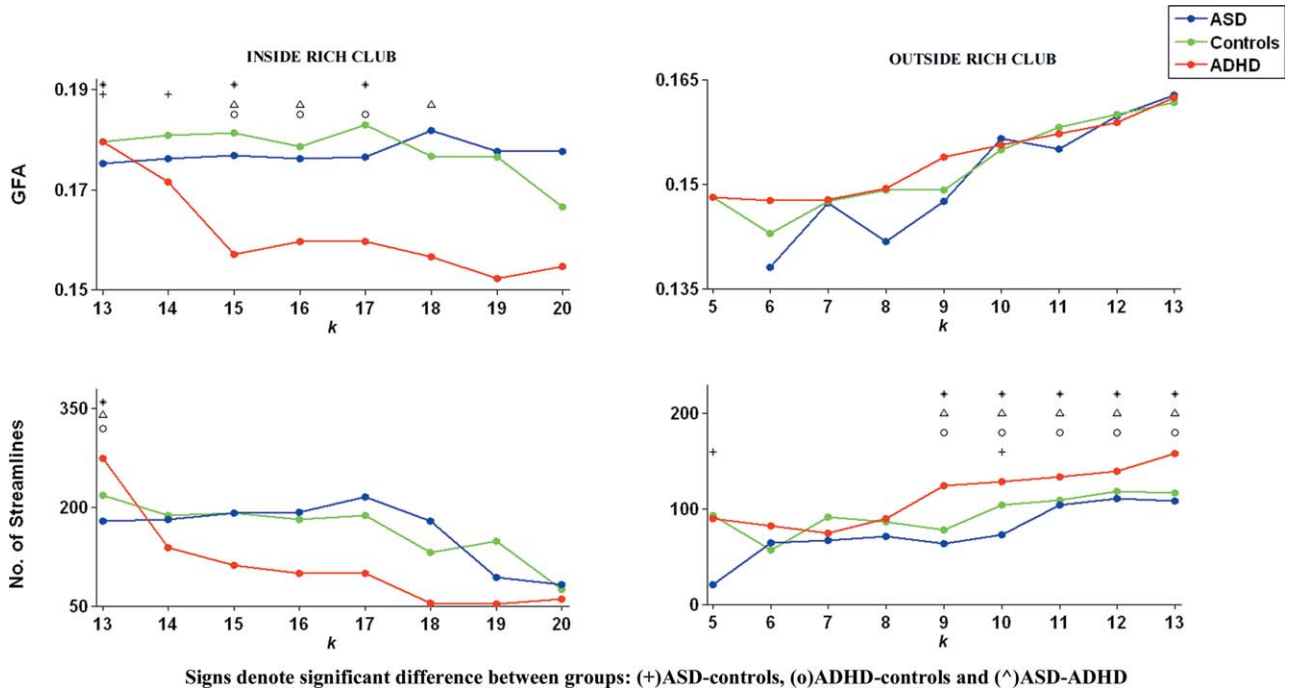

Figure 4.

GFA and number of streamlines comparison between ASD, TD, and ADHD for networks inside and outside the rich-club organization. Graphs on the top row shows the GFA-mean comparison between ASD (colored blue), controls (colored green), and ADHD group (colored red) inside and outside rich club, respectively. Graphs on the bottom row show mean of number of fiber streamlines comparison between the TD, the ASD, and the ADHD groups inside and outside the rich-club organization. Significant differences between ASD-controls are marked with "+" sign, ADHD-controls are marked with "o" sign, ASD-ADHD are marked with "^" sign and between all three groups are marked with "*" sign.

In addition, Figure 4 (in bottom left and bottom right graphs) shows the average number of streamlines measured inside and outside the rich-club organization. While we observed a reduced number of streamlines inside the rich club for the ADHD group, this finding did not reach significance. We did, however, observed more streamlines in the ADHD group outside the rich club.

Functional

Rich-club organization

Like the structural data, all three groups showed the existence of significant rich-club organization in their functional networks (Fig. 5). The regions in the functional rich-club organization in TD group were distributed bilaterally and comprises regions superior frontal, insula, anterior cingulate, paracentral, fusiform, middle temporal, and precuneus. Children with ASD showed similar rich-club regions with some extension along inferior parietal cortex, with some narrowing along superior frontal and cingulate regions. Children with ADHD also showed similar rich-club regions albeit narrowed along superior frontal, while extended along posterior cingulate and frontal pole (Fig. 6). The ϕ_{norm}comparison between the groups showed higher phi value in the ASD group at higher k-levels than the TD and ADHD groups, which was consistent with the structural network, and suggests over-connectivity in the ASD group (Supporting Information Fig. 7). Figure 6 shows the rich-club regions with $k \geq 11$ on an averaged brain surface and the corresponding spring embedded graphs for the three groups. In addition to the Maslov–Sneppen method of network rewiring, we also observed the existence of significant rich-club organization in functional networks, normalized using H-Q-S method (Supporting Information Fig. 8).

Higher connectedness coefficients in ASD inside rich-club organization

Connectedness coefficients were computed for networks inside and outside the rich-club organization. Like the structural data, both unweighted and weighted coefficients showed higher connectedness in the ASD inside the rich-club organization and no difference outside the rich-club organization, suggesting that the high functional connectedness is specific within the rich-club nodes (Fig. 7). In addition, we observed lower connectedness inside the

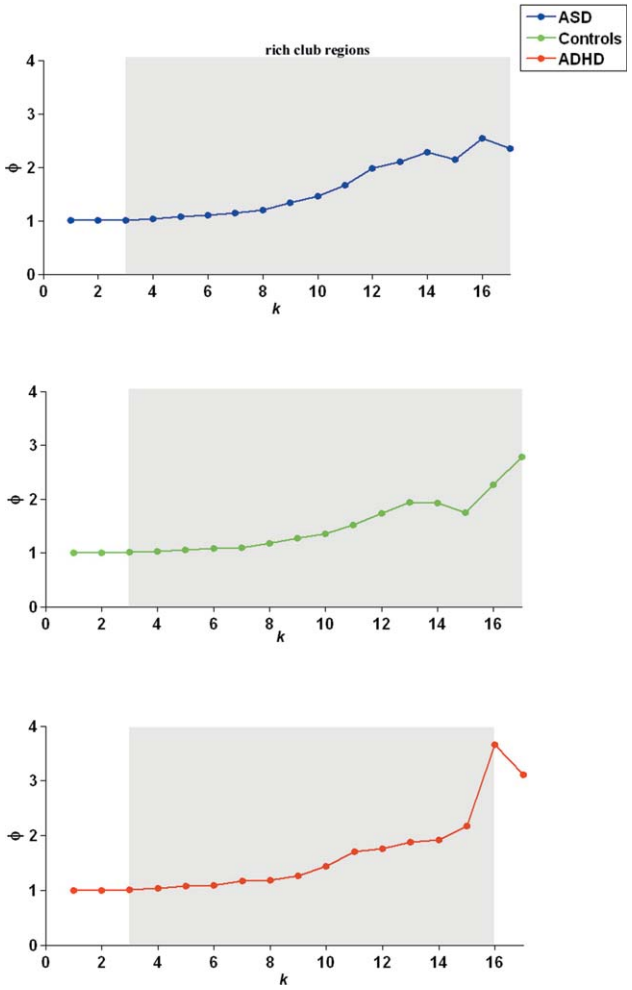

Figure 5.

Rich-club organization in functional group networks of ASD, controls, and ADHD. Rich-club coefficients normalized relative to random are shown in blue (ASD), green (controls), and red (ADHD) colors. The coefficients are plotted against degree, between 1 and 17. Shaded regions show the significant ($p < 0.05$) higher coefficients.

rich-club organization in the ADHD group, with no significant difference outside the rich-club organization. The results were also tested on correlation matrix with 6% connection density (Supporting Information Fig. 9).

Higher connectedness coefficients in ASD inside rich-club consistent in ABIDE data

To validate the higher connectedness in ASD group inside the rich-club organization, we analyzed the connectedness coefficients in a large dataset of 85 ASD and 101 TD subjects (Supporting Information Table 3), within the same age range from the ABIDE dataset [Di Martino et al., 2014]. For 3% connection density, the results were similar with ASD group characterized by higher connectedness coefficient than TD and specifically just inside the rich-club organization (shown in Fig. 8). The results were also validated on functional matrix with 6% and 9% connection density.

High correlation values in ADHD outside rich club

Consistent with the number of streamlines in structural data, the ADHD group showed a significantly higher correlation value than did the ASD and the TD groups outside the rich-club organization (shown in Fig. 9). We did not observe any significant differences between groups inside the rich club. These results were consistent with the 6% and 9% connection densities for functional matrices.

DISCUSSION

Our goal was to apply a novel approach to identifying differences in structural and functional connectivity patterns in individuals with ASD and ADHD. This approach may allow for a clearer understanding of functional and structural neurobiology underlying these conditions. The approach may also help clarify the inconsistency in the literature with respect to patterns of connectivity in neurodevelopmental disorders. Results from both structural and functional analyses converged on a striking pattern: the ASD group was characterized by over-connectivity inside the rich club, while the ADHD group was characterized by under-connectivity inside the rich club. Low GFA-mean values (and corresponding functional correlations) appeared to be, in part, responsible for the low rich-club connectivity in ADHD. Conversely, the increased connectivity in ASD was not accompanied by increased GFA, but rather by increased number of connections, suggesting a unique correlate corresponding to the increased rich-club connectivity in ASD. Interestingly, in ASD, the functional connections inside the rich club, despite being more numerous, were actually weaker in magnitude than TD.

The present results may assist in clarifying inconsistent findings in the literature with regard to ASD and ADHD. For example, the idea of an over-connectivity syndrome in ASD, at least in early life, has a long history [see Courchesne and Pierce, 2005; Wass, 2011]. Here, we show findings in middle childhood and early adolescence that are consistent with this notion both structurally and functionally; however, the novelty here is that this finding is specific to connections within the rich-club nodes themselves. The inclusion of right supramarginal region inside the rich-club organization in the ASD group may correspond to greater gray matter thickness [Brieber et al., 2007]. Outside of the rich club, findings are more consistent and support reduced connectivity in ASD at a certain point in development [Di Martino et al., 2014]. Importantly, FA values were not different relative to controls for the ASD group either within or outside of the rich club. This

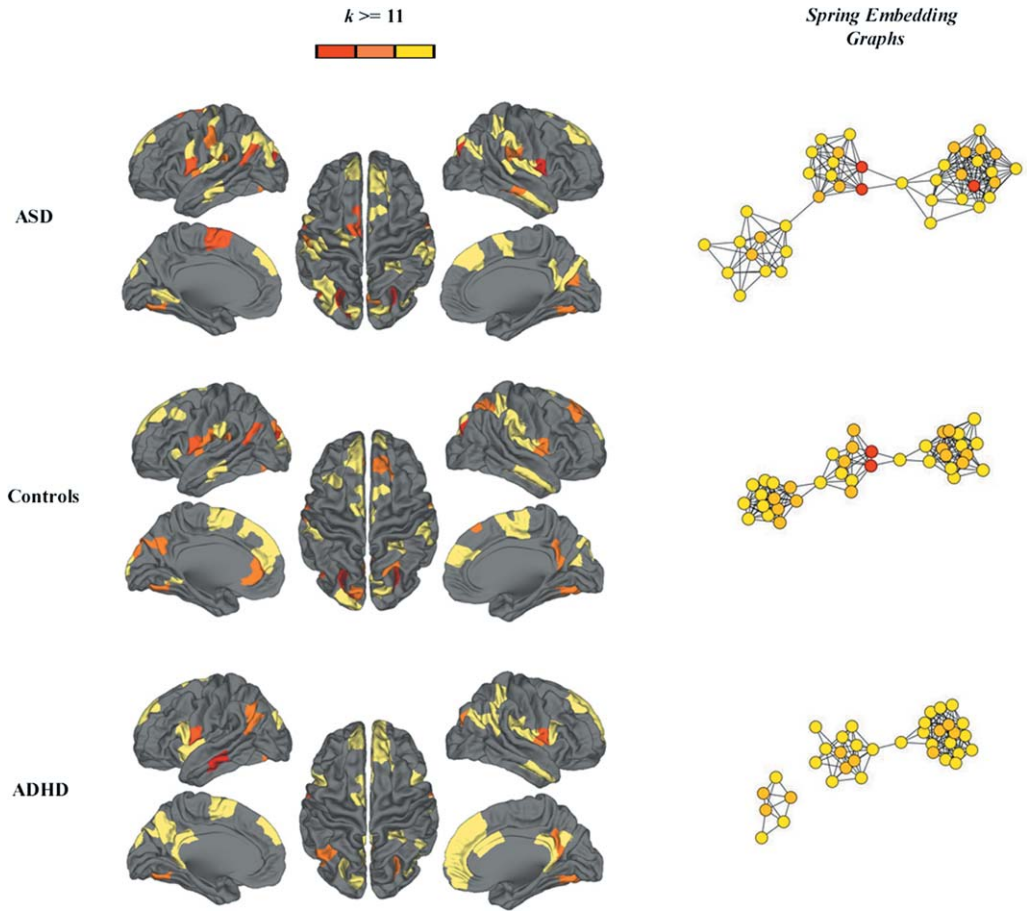

Figure 6.

Spatial topography and spring embedded graphs of functional rich club in ASD, control, and ADHD (top–bottom). Rich-club regions at $k \geq 11$ are shown for all three groups. Regions are colored based on their degree distribution (yellow to red). On the right-hand side are the spring embedded graphs for each group where regions are depicted as circles and links between them are the solid lines between them.

finding suggests that increased structural connectivity in the ASD group was not simply a result of increased sensitivity to tractography methods. In other words, tractography measurements rely on consistent and directionally oriented water diffusion. It can be argued that increased and more consistent FA values along a given tract allow that tract to be more easily identified via any given tractography algorithm. Here, relative to controls, the FA values were similar in the ASD group and not increased relative to controls, suggesting that the increased connectivity is in the form of number of tracts and streamlines were not simply a sensitivity issue with respect to the tractography methods, but an actual increase in the number of projections—a finding consistent with recent histological studies [Courchesne and Pierce, 2005; Rudie et al., 2013].

Importantly, the structural and functional connectivity findings were consistent in identifying that the number of connections between rich-club nodes is increased in ASD—findings consistent with some work in the current literature [Keown et al., 2013; Monk et al., 2009; Supekar et al., 2013; Uddin et al., 2013]. However, this increase in the number of fibers does not result in increased correlation strengths with regard to functional connectivity. Rather, overall functional correlation coefficients are decreased in ASD, which would imply that this atypical organization in the ASD population leads to disordered and inefficient communication between regions. This particular finding may be highlighting why simply comparing TD with ASD populations across many functional connections shows reduced connectivity overall [Di Martino et al., 2011] when the actual number of connections that exists is actually higher.

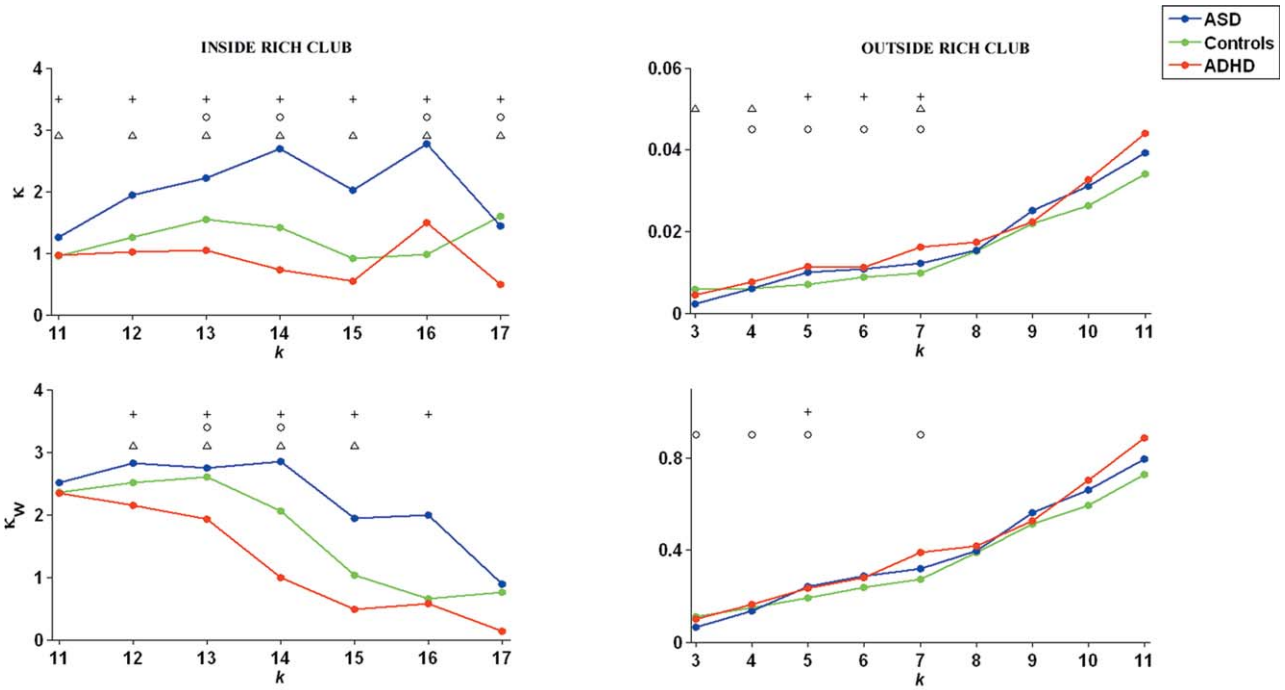

Figure 7.

Connectedness coefficients comparison between functional networks of ASD, controls, and ADHD for networks inside and outside the rich-club organization. Graphs on left-hand side shows the unweighted connectedness coefficients, weighted coefficients, and number stream lines comparison between groups inside the rich club ($11 \leq k \leq 17$), whereas right-hand side graphs shows these comparison for networks outside the rich club ($3 \leq k \leq 11$). Significant differences between ASD-controls are marked with "+" sign, ADHD-controls are marked with "o" sign, ASD-ADHD are marked with "^" sign.

Findings in the ADHD group were distinct from the ASD group in many ways. In the ADHD group, our findings of lower levels of structural and functional connectivity (Supporting Information Figures 4 and 7) inside rich-club networks demonstrates that although these rich-club regions are highly connected regions in the network, the connectivity among these regions is reduced. Moreover, lower GFA-mean values for networks within the rich club explained this lower connectivity inside the rich-club network. Here, as opposed to the ASD findings, the reduced FA values in ADHD may be highlighting reduced ability for the tractography algorithms to identify tracts and streamlines. Thus, it is not clear whether reduced connectivity within the rich club is a result of reduced sensitivity due to lower FA in ADHD, reduced underlying structural connectivity, or both. Nonetheless, our findings suggest that reduced FA and structural and functional connectivity highlighted in the literature with regard to ADHD are specific to the rich-club nodes. Importantly, however, the ADHD group was not simply characterized by reduced connectivity. Rather, outside the rich club this population had a higher number of streamlines and correlation values demonstrating the marked complexity of the network dynamics within this disorder.

Although ADHD and ASD commonly co-occur [Rommelse et al., 2011], share some degree of common familial/genetic influences [Musser et al., 2014; Rommelse et al., 2010; Ronald et al., 2008], and share common impairments [e.g., some aspects of executive functioning, see Pennington and Ozonoff, 1996], our findings identify mostly distinct connectivity patterns between the two syndromes with regard to brain-wide network organization. These findings may have important implications for the manner in which these two conditions are conceptualized. Our findings relate to a recent report by Di Martino et al [Di Martino et al., 2014], that showed distinct connectivity patterns, in some subcortical regions, and shared patterns in the precuneus with regard to degree centrality in ASD and ADHD. It is important to note however, that our analysis is based on specific cortical ROIs, which is distinct from a voxelwise analyses of this type. While there continue to be debate on how best to characterize network characteristics using functional data [Hagmann et al., 2012], using voxels as nodes in a graph (or even many small ROIs) can lead to network statistics that are biased based on the size of the underlying area in which they are located [Hagmann et al., 2012; Power et al., 2011, 2012]. For example, if one

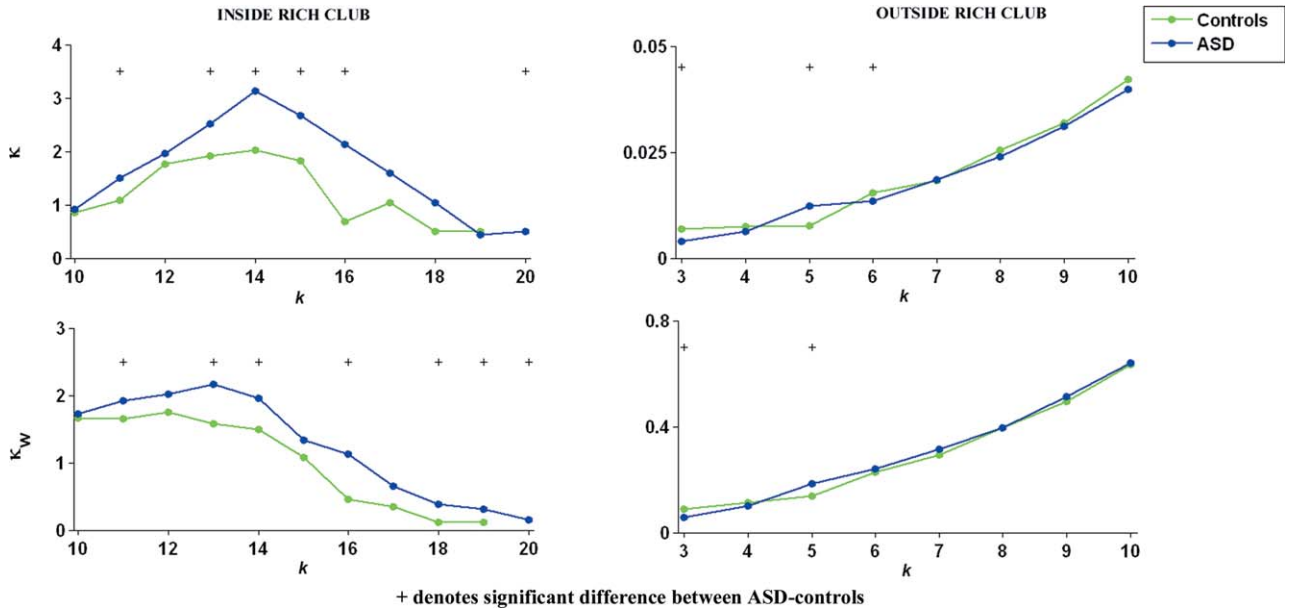

Figure 8.

Connectedness coefficients comparison between functional networks of ASD and controls (ABIDE data) for networks inside and outside the rich-club organization. The left-hand side graphs shows the unweighted connectedness coefficients and weighted coefficients comparison between groups inside the rich club ($11 \leq k \leq 17$), the right-hand side graphs shows these comparison for networks outside the rich club ($3 \leq k \leq 11$). Significant differences between ASD-controls are marked with "+" sign.

has several regions or voxels that reside inside a relatively large functional area, many measures of centrality can be artificially skewed high simply because of the many voxels/regions within the area are essentially connecting with themselves [Hagmann et al., 2012; Power et al., 2011, 2012]. In addition, we note that while the results are not identical our findings do not to suggest that no overlapping atypical circuit characteristics exist between these populations, but rather that large-scale topological organization, as measured via the rich club, is in many ways distinct. However, the absence of left medial temporal gyrus from the structural rich-club organization in ADHD group (see Fig. 2) may associate with gray matter reduction in the two groups [Brieber et al. 2007] and reduced left

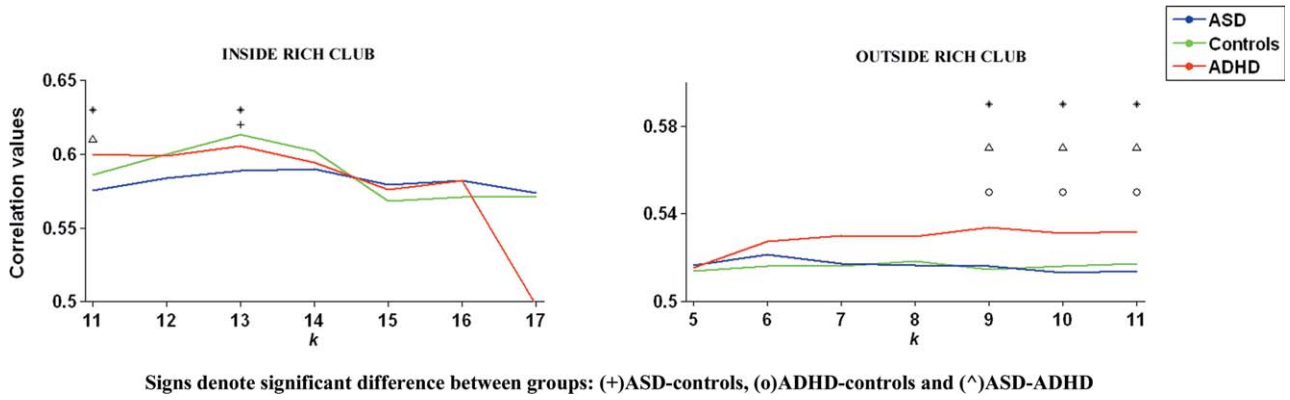

Figure 9.

Correlation values comparison between ASD, TD, and ADHD group inside and outside rich-club organization. Average of correlation values across various degree levels are compared between ASD (blue), TD (green), and ADHD (red). Significant difference, from ANOVA, are marked using "*". Significant differences between ASD-controls are marked with "+" sign, ADHD-controls are marked with "o" sign, ASD-ADHD are marked with "^" sign.

dorsolateral prefrontal cortex in the functional rich club in ADHD and ASD groups than in TD might be associated with the underactivation of the region in the two disorders [Christakou et al., 2013].

LIMITATIONS

This study opens a potential new way of thinking about the ADHD-ASD relation, but key limitations should be noted. First is the small sample size of ASD and ADHD subjects. While the findings from the structural data and functional data were robust and consistent in the current sample, and were reproduced using the functional data from the ABIDE consortium (which included 85 ASD and 101 TD subjects), the small sample sizes does increase the risk of Type II errors. Second, the work does not address the marked heterogeneity that resides within each of these disorders. It is likely, if not already empirically demonstrated [Fair et al., 2013; Gates et al., 2014; Karalunas et al., 2014], that these populations encompass multiple subpopulations with unique underlying brain physiology. Thus, the current findings should be considered preliminary in that regard. Some of the findings here are likely to be consistent across the disordered populations, or at the least be present in a large portion of those affected. Seeing how the identified effects stratify across ASD populations comorbid with ADHD [APA, 2013] will be of particular interest. Third, region selection is an important issue when using graph theory approaches to study brain connectivity as results may change depending on number of regions, regions size, and their location on cortex. Ideally regions should be selected based on functionally segregated units [Barnes et al., 2010; Cohen et al., 2008; Hagmann et al., 2012] or areas; unfortunately, identifying a complete collection of these units in human brain is still out of reach. Replicating the current findings in alternative parcellation schemes will be important in future work. Lastly, the ASD group includes two subjects who were diagnosed based on clinic determination, as opposed to a research reliable diagnosis in the laboratory [see Supporting Information Table 1(b)]. While this would be more likely to lead to Type II than Type I error, replication with larger, carefully diagnosed samples is needed.

CONCLUSIONS

Overall, the present investigation identified distinct patterns of connectivity between ASD and ADHD using a novel approach. Because it has previously proven elusive to identify consistent, distinct differential patterns that characterize ASD versus ADHD across multiple domains, it has been suggested that ADHD and ASD may be different manifestations of the same disorder [Rommelse et al., 2011]. This study identified distinct patterns of connectivity in ASD versus ADHD, suggesting that there may be distinct neural mechanisms underlying the expression of each syndrome. How these distinct patterns differentially relate to specific symptom domains will be an important area for future research. Additionally, whether structural and functional connectivity patterns may constitute endophenotypes is a critical question to continue to attempt to address. Identifying endophenotypes and shared versus distinct etiological factors are crucial steps toward understanding the complex genetic susceptibility and etiologic heterogeneity for both ADHD and ASD [Castellanos and Tannock, 2002; Rommelse et al., 2011]. Simultaneous evaluation of both functional and structural brain measures in ASD and ADHD has been proposed as an important aspect of this effort [Rommelse et al., 2011]. Further research in this area may have important implications for our conceptualization, classification, and treatment of neurodevelopmental disorders.

REFERENCES

American Psychiatric Association (2000): Diagnostic and Statistical Manual of Mental Disorders, 4th ed. Washington, DC: American Psychiatric Press.

American Psychiatric Association (2013): Diagnostic and Statistical Manual of Mental Disorders, 5th ed. Arlington, VA: American Psychiatric Press.

Anderson JS, Druzgal TJ, Froehlich A, DuBray MB, Lange N, Alexander AL, Abildskov T, Nielsen JA, Cariello AN, Cooperrider JR, Bigler ED, Lainhart JE (2011): Decreased interhemispheric functional connectivity in autism. Cereb Cortex 21:1134–1146.

Aoki Y, Abe O, Nippashi Y, Yamasue H (2013): Comparison of white matter integrity between autism spectrum disorder subjects and typically developing individuals: A meta-analysis of diffusion tensor imaging tractography studies. Mol Autism 4.

Assaf M, Jagannathan K, Calhoun VD, Miller L, Stevens MC, Sahl R, O'Boyle JG, Schultz RT, Pearlson GD (2010): Abnormal functional connectivity of default mode sub-networks in autism spectrum disorder patients. Neuroimage 53:247–256.

Barnes KA, Cohen AL, Power JD, Nelson SM, Dosenbach YB, Miezin FM, Petersen SE, Schlaggar BL (2010): Identifying Basal Ganglia divisions in individuals using resting-state functional connectivity MRI. Front Syst Neurosci 4.

Bassett DS, Bullmore ET (2009): Human brain networks in health and disease. Curr Opin Neurol 22:340–347.

Boyle CA, Boulet S, Schieve L, Cohen RA, Blumberg SJ, Yeargin-Allsopp M, Visser S, Kogan MD (2011): Trends in the prevalence of developmental disabilities in US children, 1997–2008. Pediatrics 127:1034–1042.

Brieber S, Neufang S, Bruning N, Kamp-Becker I, Remschmidt H, Herpertz-Dahlmann B, Fink GR, Konrad K (2007): Structural brain abnormalities in adolescents with autism spectrum disorder and patients with attention deficit/hyperactivity disorder. J Child Psychol Psychiatry 48:1251–1258.

Castellanos FX, Tannock R (2002): Neuroscience of attention-deficit/hyperactivity disorder: The search for endophenotypes. Nat Rev Neurosci 3:617–628.

Cherkassky VL, Kana RK, Keller TA, Just MA (2006): Functional connectivity in a baseline resting-state network in autism. Neuroreport 17:1687–1690.

Cheung C, Chua SE, Cheung V, Khong PL, Tai KS, Wong TK, Ho TP, McAlonan GM (2009): White matter fractional anisotrophy

differences and correlates of diagnostic symptoms in autism. J Child Psychol Psychiatry 50:1102–1112.

Christakou A, Murphy CM, Chantiluke K, Cubillo AI, Smith AB, Giampietro V, Daly E, Ecker C, Robertson D, MRC AIMS consortium, Murphy DG, Rubia K (2013): Disorder-specific functional abnormalities during sustained attention in youth with Attention Deficit Hyperactivity Disorder (ADHD) and with autism. Mol Psychiatry 18:236–244.

Cohen AL, Fair DA, Miezin FM, Dosenbach NU, Schlaggar BL, Petersen SE (2008): Defining functional areas in individual human brains using resting functional connectivity MRI. Neuroimage 41:45–57.

Colizza V, Flammini A, Serrano MA, Vespignani A (2006): Detecting rich-club ordering in complex networks. Nat Phys 2:110–115.

Courchesne E, Pierce K (2005): Why the frontal cortex in autism might be talking only to itself: Local over-connectivity but long-distance disconnection. Curr Opin Neurobiol 15:225–230.

Di Martino A, Kelly C, Grzadzinski R, Zuo X-N, Mennes M, Mairena MA, Lord C, Castellanos FX, Milham MP (2011): Aberrant striatal functional connectivity in children with autism. Biol Psychiatry 69:847–856.

Di Martino A, Yan C-G, Li Q, Denio E, Castellanos FX, Alaerts K, Anderson JS, Assaf M, Bookheimer SY, Dapretto M, Deen B, Delmonte S, Dinstein I, Ertl-Wagner B, Fair DA, Gallagher L, Kennedy DP, Keown CL, Keysers C, Lainhart JE, Lord C, Luna B, Menon V, Minshew NJ, Monk CS, Mueller S, Muller RA, Nebel MB, Nigg JT, O'Hearn K, Pelphrey KA, Peltier SJ, Rudie JD, Sunaert S, Thioux M, Tyszka JM, Uddin LQ, Verhoeven JS, Wenderoth N, Wiggins JL, Mostofsky SH, Milham MP (2014): The autism brain imaging data exchange: Towards a large-scale evaluation of the intrinsic brain architecture in autism. Mol Psychiatry 19:659–667.

Dinstein I, Pierce K, Eyler L, Solso S, Malach R, Behrmann M, Courchesne E (2011): Disrupted neural synchronization in toddlers with autism. Neuron 70:1218–1225.

Ebisch SJH, Gallese V, Willems RM, Mantini D, Groen WB, Romani GL, Buitelaar JK, Bekkering H (2011): Altered intrinsic functional connectivity of anterior and posterior insula regions in high-functioning participants with autism spectrum disorder. Hum Brain Mapp 32:1013–1028.

Fair DA, Posner J, Nagel BJ, Bathula D, Dias TGC, Mills K, Blythe MS, Giwa A, Schmitt CF, Nigg JT (2010): Atypical default network connectivity in youth with attention-deficit/hyperactivity disorder. Biol Psychiatry 68:1084–1091.

Fair DA, Nigg JT, Iyer S, Bathula D, Mills KL, Dosenbach NUF, Schlaggar BL, Mennes M, Gutman D, Bangaru S, Buitelaar JK, Dickstein DP, DiMartino A, Kennedy DN, Kelly C, Luna B, Schweitzer JB, Velanova K, Wang YF, Mostofsky S, Castellanos FX, Milham MP (2013): Distinct neural signatures detected for ADHD subtypes after controlling for micro-movements in resting state functional connectivity MRI data. Front Syst Neurosci 6.

Fox MD, Snyder AZ, Vincent JL, Corbetta M, Essen DCV, Raichle ME (2005): The human brain is intrinsically organized into dynamic, anticorrelated functional networks. Proc Natl Acad Sci USA 102:9673–9678.

Gates KM, Molenaar PCM, Iyer SP, Nigg JT, Fair DA (2014): Organizing heterogeneous samples using community detection of GIMME-derived resting state functional networks. PLoS One 9(3):e91322.

Geurts HM, Verte S, Oosterlaan J, Roeyers H, Sergeant JA (2004): How specific are executive functioning deficits in attention deficit hyperactivity disorder and autism? J Child Psychol Psychiatry 45:836–854.

Gotts SJ, Simmons WK, Milbury LA, Wallace GL, Cox RW, Martin A (2012): Fractionation of social brain circuits in autism spectrum disorders. Brain 135:2711–2725.

Grayson DS, Ray S, Carpenter S, Iyer S, Dias TGC, Stevens C, Nigg JT, Fair DA (2014): Structural and functional rich club organization of the brain in children and adults. PLoS One 9: e88297.

Hagmann P, Cammoun L, Gigandet X, Meuli R, Honey CJ, Wedeen VJ, Sporns O (2008): Mapping the Structural Core of Human Cerebral Cortex. PLoS Biol 6:e159.

Hagmann P, Grant PE, Fair DA (2012): MR connectomics: A conceptual framework for studying the developing brain. Front Syst Neurosci 6.

Hallquist MN, Hwang K, Luna B (2013): The nuisance of nuisance regression: Spectral misspecification in a common approach to resting-state fMRI preprocessing reintroduces noise and obscures functional connectivity. Neuroimage 82:208–225.

Happé F, Ronald A, Plomin R (2006): Time to give up on a single explanation for autism. Nat Neurosci 9:1218–1220.

Karalunas SL, Geurts HM, Konrad K, Bender S, Nigg JT (2014): Annual Research Review: Reaction time variability in ADHD and autism spectrum disorders: Measurement and mechanisms of a proposed trans-diagnostic phenotype. J Child Psychol Psychiatry 55:685–710.

Kaufman J, Birmaher B, Brent D, Rao U, Flynn C, Moreci P, Williamson D, Ryan N (1997): Schedule for affective disorders and schizophrenia for school-age children-present and lifetime version (K-SADS-PL): Initial reliability and validity data. J Am Acad Child Adoles Psychiatry 36:980–988.

Kennedy DP, Courchesne E (2008): The intrinsic functional organization of the brain is altered in autism. Neuroimage 39:1877–1885.

Keown CL, Shih P, Nair A, Peterson N, Mulvey ME, Müller R-A (2013): Local functional overconnectivity in posterior brain regions is associated with symptom severity in autism spectrum disorders. Cell Rep 5:567–572.

Lord C, Rutter M, LeCouteur A (1994): Autism diagnostic interview-revised: A revised version of a diagnostic interview for caregivers of individuals with possible pervasive developmental disorders. J Autism Dev Disord 24:659–685.

Lord C, Risi S, Lambrecht L, Cook EH Jr, Leventhal BL, DiLavore PC, Pickles A, Rutter M (2000): The autism diagnostic observation schedule-generic: A standard measure of social and communication deficits associated with the spectrum of autism. J Autism Dev Disord 30:205–223.

Lynch CJ, Uddin LQ, Supekar K, Khouzam A, Phillips J, Menon V (2013): Default mode network in childhood autism: Posteromedial cortex heterogeneity and relationship with social deficits. Biol Psychiatry 74:212–219.

Maslov S, Sneppen K (2002): Specificity and stability in topology of protein networks. Science 296:910–913.

Monk CS, Peltier SJ, Wiggins JL, Weng SJ, Carrasco M, Risi S, Lord C (2009): Abnormalities of intrisic functional connectivity in autism spectrum disorders. Neuroimage 47:764–772.

Mori S, Zhang J (2006): Principles of diffusion tensor imaging and its applications to basic neuroscience research. Neuron 51:527–539.

Mueller S, Keeser D, Samson AC, Kirsch V, Blautzik J, Grothe M, Erat O, Hegenloh M, Coates U, Reiser MF, Hennig-Fast K, Meindl T (2013): Convergent findings of altered functional and structural brain connectivity in individuals with high functioning autism: A multimodal MRI study. PLoS One 8.

Musser ED, Hawkey E, Kachan-Liu SS, Lees P, Roullet J-B, Goddard K, Steiner RD, Nigg JT (2014): Shared familial transmission of autism spectrum and attention-deficit/hyperactivity disorders. J Child Psychol Psychiatry 55:819–827.

Nagel BJ, Bathula D, Herting M, Schmitt C, Kroenke CD, Fair D, Nigg JT (2011): Altered white matter microstructure in children with attention-deficit/hyperactivity disorder. J Am Acad Child Adolesc Psychiatry 50:283–292.

Opsahl T, Colizza V, Panzarasa P, Ramasco JJ (2008): Prominence and control: The weighted rich-club effect. Phys Rev Lett 101.

Pavuluri MN, Yang S, Kamineni K, Passarotti AM, Srinivasan G, Harral EM, Sweeney JA, Zhou XJ (2009): Diffusion tensor imaging study of white matter fiber tracts in pediatric bipolar disorder and attention-deficit/hyperactivity disorder. Biol Psychiatry 65:586–593.

Pennington BF, Ozonoff S (1996): Executive functions and developmental psychopathology. J Child Psychol Psychiatry 37: 51–87.

Peterson BS, Potenza MN, Wang ZS, Zhu HT, Martin A, Marsh R, Plessen KJ, Yu S (2009): An fMRI study of the effects of psychostimulants on default-mode processing during Stroop task performance in youths with ADHD. Am J Psychiatry 166: 1286–1294.

Power JD, Cohen AL, Nelson SM, Wig GS, Barnes KA, Church JA, Vogel AC, Laumann TO, Miezin FM, Schlaggar BL, Petersen SE (2011): Functional Network Organization of the Human Brain. Neuron 72:665–678.

Power JD, Barnes KA, Snyder AZ, Schlaggar BL, Petersen SE (2012): Spurious but systematic correlations in functional connectivity MRI networks arise from subject motion. Neuroimage 59:2142–2154.

Rommelse NNJ, Franke B, Geurts HM, Hartman CA, Buitelaar JK (2010): Shared heritability of attention-deficit/hyperactivity disorder and autism spectrum disorder. Eur Child Adolesc Psychiatry 19:281–295.

Rommelse NNJ, Geurts HM, Franke B, Buitelaar JK, Hartman CA (2011): A review on cognitive and brain endophenotypes that may be common in autism spectrum disorder and attention-deficit/hyperactivity disorder and facilitate the search for pleiotropic genes. Neurosci Biobehav Rev 35:1363–1396.

Ronald A, Simanoff E, Kuntsi J, Asherson P, Plomin R (2008): Evidence for overlapping genetic influences on autistic and ADHD behaviours in a community twin#sample. J Child Psychol Psychiatry 49:535–542.

Rudie JD, Hernandez LM, Brown JA, Beck-Pancer D, Colich NL, Gorrindo P, Thompson PM, Geschwind DH, Bookheimer SY, Levitt P, Dapretto M (2012): Autism-associated promoter variant in MET impacts functional and structural brain networks. Neuron 75, 904–915.

Rudie JD, Brown JA, Beck-Pancer D, Hernandez LM, Dennis EL, Thompson PM, Bookheimer SY, Dapretto M (2013): Altered functional and structural brain network organization in autism. NeuroImage: Clinical 2:79–94.

Silk TJ, Vance A, Rinehart N, Bradshaw JL, Cunnington R (2009): White-matter abnormalities in attention deficit hyperactivity disorder: A diffusion tensor imaging study. Hum Brain Mapp 30:2757–2765.

Sinzig J, Morsch D, Bruning N, Schmidt MH, Lehmkuhl G (2008): Inhibition, flexibility, working memory and planning in autism spectrum disorders with and without comorbid ADHD-symptoms. Child Adolesc Psychiatry Ment Health 2.

Supekar K, Uddin LQ, Khouzam A, Phillips J, Gaillard WD, Kenworthy LE, Yerys BE, Vaidya CJ, Menon V (2013): Brain hyperconnectivity in children with autism and its links to social deficits. Cell Rep 5:738–747.

Tien L, Jiang T, Wang Y, Zang Y, He Y, Liang M, Sui M, Cao Q, Hu S, Peng M, Zhuo Y (2006): Altered resting-state functional connectivity patterns of anterior cingulate cortex in adolescents with attention deficit hyperactivity disorder. Neurosci Lett 400: 39–43.

Tomasi D, Volkow ND (2012): Abnormal functional connectivity in children with attention-deficit/hyperactivity disorder. Biol Psychiatry 71:443–450.

Tuch DS (2004): Q-ball imaging. Magn Reson Med 52:1358–1372.

Uddin LQ, Supekar K, Lynch CJ, Khouzam A, Phillips J, Feinstein C, Ryali S, Menon V (2013): Salience network–based classification and prediction of symptom severity in children with autism. JAMA Psychiatry 70, 869–879.

Uddin LQ, Kelly AMC, Biswal BB, Marguiles DS, Shehzad Z, Shaw D, Ghaffari M, Rotrosen J, Adler LA, Castellanos FX, Milham MP (2008): Network homogeneity reveals decreased integrity of default-mode network in ADHD. J Neurosci Methods 169:249–254.

van den Heuvel MP, Sporns O (2011): Rich-club organization of the human connectome. J Neurosci 31:15775–15786.

van den Heuvel MP, Mandl RCW, Stam CJ, Kahn RS, Pol HEH (2010): Aberrant frontal and temporal complex network structure in schizophrenia: A graph theoretical analysis. J Neurosci 30:15915–15926.

van den Heuvel MP, Kahn RS, Goñi J, Sporns O (2012): High-cost, high-capacity backbone for global brain communication. Proc Natl Acad Sci USA 109:11372–11377.

van Ewijk H, Heslenfeld DJ, Zwiers MP, Buitelaar JK, Oosterlaan J (2012): Diffusion tensor imaging in attention deficit/hyperactivity disorder: A systematic review and meta-anlysis. Neurosci Biobehav Rev 36:1093–1106.

van Wijk BCM, Stam CJ, Daffertshofer A (2010): Comparing brain networks of different size and connectivity density using graph theory. PLoS One 5.

von dem Hagen EA, Stoyanova RS, Baron-Cohen S, Calder AJ (2012): Reduced functional connectivity within and between 'social' resting state networks in autism spectrum conditions. Soc Cogn Affect Neurosci 8:694–701.

Washington SD, Gordon EM, Brar J, Warburton S, Sawyer AT, Wolfe A, Mease-Ference ER, Girton L, Hailu A, Mbwana J, Gaillard WD, Kalbfleisch ML, Vanmeter JW (2014): Dysmaturation of the default mode network in autism. Hum Brain Mapp 35:1284–1296.

Wass S (2011): Distortions and disconnections: disrupted brain connectivity in autism. Brain Cogn 75:18–28.

Weng S, Wiggins JL, Peltier SJ, Carrasco M, Risi S, Lord C, Monk CS (2010): Alterations of resting state functional connectivity in the default network in adolescents with autism spectrum disorders. Brain Res 1313:202–214.

Zalesky A, Fornito A, Bullmore E (2012): On the use of correlation as a measure of network connectivity. Neuroimage 60:2096–2106.

Zhou S, Mondragon RJ (2004): The rich-club phenomenon in the Internet topology. IEEE Comm Lett 8:180–182.